Fluidity of the system produced in relativistic pp and heavy-ion collisions: Hadron resonance gas model approach

Ronald Scaria[1], Dushmanta Sahu[1], Captain R. Singh[1], Raghunath Sahoo[1,2*], and Jan-e Alam[3]
[1] *Department of Physics, Indian Institute of Technology Indore, Simrol, Indore 453552, India*
[2] *CERN, CH 1211, Geneva 23, Switzerland and*
[3] *Variable Energy Cyclotron Centre, 1/AF, Bidhan Nagar, Kolkata, India*
(Dated: June 27, 2023)

We have estimated the dimensionless parameters such as Reynolds number (Re), Knudsen number (Kn) and Mach number (Ma) for a multi-hadron system by using the excluded volume hadron resonance gas (EVHRG) model along with Hagedorn mass spectrum to include higher resonances in the system. The size dependence of these parameters indicate that the system formed in proton+proton collisions may achieve thermal equilibrium making it unsuitable as a benchmark to analyze the properties of the system produced in heavy ion collisions at similar energies. While the magnitude of Kn can be used to study the degree of thermalization and applicability of inviscid hydrodynamics, the variations of Re and Ma with temperature (T) and baryonic chemical potential (μ_B) assist to understand the change in the nature of the flow in the system. Indeed the nature of flow changes from laminar to turbulent as Re increases and the system is characterized as incompressible for low $Ma(<< 1)$ and compressible for larger Ma. Ma can also be used to understand whether the flow is subsonic or supersonic.

PACS numbers:

arXiv:2201.08096v2 [hep-ph] 26 Jun 2023

I. INTRODUCTION

Relativistic heavy-ion collisions aim to create extreme conditions of temperature (T) and baryonic chemical potential (μ_B) so as to melt the hadrons to produce a deconfined state of quarks and gluons, called Quark-Gluon Plasma (QGP). Although initially it was envisaged that such a state of matter would behave as an ideal gas, the analysis of the results from the nuclear collisions at the Relativistic Heavy-Ion Collider (RHIC) and Large Hadron Collider (LHC) energies reveal that the created matter behaves like strongly interacting liquid with low shear viscosity (η) to entropy density (s) ratio. The study of experimental data within the framework of relativistic hydrodynamics shows that the η/s of QGP is close to $1/4\pi$, which is the AdS/CFT bound obtained in Ref. [1], indicating the creation of a "perfect fluid" in relativistic heavy-ion collisions at the RHIC [2–5]. So far, the results from proton+proton (pp) collisions were used as a baseline for establishing QCD medium formation in heavy-ion collisions at RHIC and LHC energies. However, recent observations of strangeness enhancement, collectivity, long-range particle correlations etc. in pp and p+Pb collisions at the LHC energies [6, 7] opened up a new domain of studies. These observations advocate for the possibility of thermalization and collectivity in the small system produced in pp collisions. Final state multiplicity dependent event characterization and collision centrality selection even in such collisions emerged out with intense search for QGP-like properties in high-multiplicity pp collisions. Although the formation of QGP-droplets is yet to be established, a detailed characterization of the system formed in pp collisions at the LHC through various theoretical models and experimental searches using new observables are underway. The study of final state event multiplicity in pp, p+Pb and heavy-ion collisions at the LHC energies, has become one of the unique observables to describe the system size and collision energy dependence of various observables. In this direction, one tries to find a threshold in the final state multiplicity [8–11] after which QGP-like properties reveal and the corresponding theoretical models to understand a QCD medium formation, including those to study thermalization and hydrodynamic models could be employed.

The possibility of thermalization in a system and the applicability of hydrodynamics can be studied using Kn. The nature of the hydrodynamic flow (laminar or turbulent) can be classified based on the magnitude of the Re and the Ma helps in determining whether the fluid is compressible or incompressible. The inequalities, $Ma << 1$ (subsonic) indicate that the fluid is incompressible and $Ma >> 1$ (supersonic) hints that it is compressible. Fluid with a high value of Re will show turbulent behavior. Kn is the ratio of the mean free path of the system to some macroscopic length scale. Therefore, small values of Kn imply a system with a small gradient of hydrodynamic quantities (see [12] and references therein) and a high degree of thermalization. A large value of Kn suggests that the system remains far away from equilibrium. In such cases fluid dynamics can still be applied with the inclusion of higher-order gradients of hydrodynamic quantities which is a very active field of contemporary research but beyond the scope of present work (see [12] for details). The Kn was estimated from a hydrodynamic model, in which the elliptic flow as a function of centrality suggests the value of

*Corresponding author: *Raghunath.Sahoo@cern.ch*

$Kn \simeq 0.3$ for central collisions and 0.5 for semi-central collisions [13, 14] of Au+Au at $\sqrt{s_{\rm NN}} = 200$ GeV. As $Re \sim \frac{inertial force}{viscous force} \sim 1/\eta$, systems with low viscosity are likely to manifest turbulent nature because in such cases perturbations in hydrodynamic quantities will grow and drive the system towards turbulent motion. At RHIC energy for a system of size 5 fm and temperature around $T = 300$ MeV, Re varies between $10-100$ for a fluid velocity in the range $0.1-1$ (in the unit of $c = 1$) [15]. Similarly, Ma is defined as the ratio of the flow velocity to the speed of sound in the system. For $Ma << 1$, the fluid density is almost uniform which suggests that the flow is incompressible. Thus, Ma can help in characterizing the compressibility of the fluid. These three parameters can be used together to achieve the following goals: (i) Kn will indicate the thermalization in the system, (ii) Re hints at the nature of the flow (laminar or turbulent) and finally (iii) Ma indicates whether the fluid is compressible ($Ma \gtrsim 1$) or incompressible ($Ma << 1$). The Ma for relativistic fluids (flow velocity close to the velocity of light) will be larger than 1 indicating that it can not be treated as incompressible. Therefore, it is expected that fluid system produced in the relativistic collision of nuclei will be compressible. The applicability of hydrodynamics (for $Kn << 1$) will give information about properties like compressibility and viscosity of the fluid [16].

To understand the thermodynamics of the system produced in ultra-relativistic collisions, inputs from lattice quantum chromodynamics (LQCD) have been extremely useful. However, it works accurately for very low baryochemical potential ($\mu_B/T \to 0$). In this context models such as Hadron Resonance Gas (HRG) can be useful to analyze data without having restrictions on the value of baryochemical potential. The HRG model has been used successfully to study the thermodynamics of the hadronic phase that appears in the course of the evolution of the system produced in ultra-relativistic collisions. In this article, we have used the HRG model with excluded volume effect along with a Hagedorn mass spectrum to study the thermal behavior of the hadronic phase formed in relativistic collisions [17–19].

This article is organized as follows. Detailed descriptions of the formalism and methodology to calculate the thermodynamic properties are given in Sec. II. In Sec. III, we present the results along with a detailed discussion. Finally, we summarize our study in Sec. IV.

II. FORMALISM

A. Hadron Resonance Gas with Excluded Volume

The hadron resonance gas model describes the hadronic phase of the matter by assuming that the system is composed of free hadrons of different species. It treats various hadrons and their resonances as point particles. However, the existence of repulsive interactions among the hadrons has already been known from the nucleon-nucleon scattering experiments. The excluded volume hadron resonance gas (EVHRG) model takes such repulsive interactions into account. The volume available for the hadrons to move is reduced by the volume that the hadrons occupy. The EVHRG model estimations for various thermodynamic quantities match the LQCD estimations up to $T \sim 140$ MeV. It is also essential to take into account the effect of the Hagedorn mass spectrum, which includes the yet unmeasured higher masses of the hadrons, as they can have a significant contribution to the Equation of State (EoS) near the critical temperature (T_c).

In a Grand Canonical Ensemble (GCE) of ideal HRG (IHRG) formalism, the partition function of the particle i can be written as [17];

$$ln Z_i^{id} = \pm \frac{V g_i}{2\pi^2} \int_0^\infty p^2 dp \; ln\{1 \pm \exp[-(E_i - \mu_i)/T]\} \quad (1)$$

where g_i and $E_i = \sqrt{p^2 + m_i^2}$ are the degeneracy and energy of the hadron i, respectively. The corresponding chemical potential is given by,

$$\mu_i = B_i \mu_B + S_i \mu_S + Q_i \mu_Q, \quad (2)$$

where B_i, S_i, and Q_i are the baryon number, strangeness, and electric charge of the i^{th} hadron. The μ_B, μ_S, μ_Q are the baryonic, strangeness and electric chemical potentials respectively. The pressure P_i, energy density ε_i, number density n_i and entropy density s_i can be obtained from the partition function by using the following relations:

$$P_i^{id}(T, \mu_i) = \pm \frac{T g_i}{2\pi^2} \int_0^\infty p^2 dp \; ln\{1 \pm \exp[-(E_i - \mu_i)/T]\} \quad (3)$$

$$\varepsilon_i^{id}(T, \mu_i) = \frac{g_i}{2\pi^2} \int_0^\infty \frac{E_i \; p^2 dp}{\exp[(E_i - \mu_i)/T] \pm 1} \quad (4)$$

$$n_i^{id}(T, \mu_i) = \frac{g_i}{2\pi^2} \int_0^\infty \frac{p^2 dp}{\exp[(E_i - \mu_i)/T] \pm 1} \quad (5)$$

$$s_i^{id}(T, \mu_i) = \pm \frac{g_i}{2\pi^2} \int_0^\infty p^2 dp \Big[\ln\{1 \pm \exp[-(E_i - \mu_i)/T]\} \pm \frac{(E_i - \mu_i)/T}{\exp[(E_i - \mu_i)/T] \pm 1} \Big] \quad (6)$$

The effect of higher states and resonances is included in IHRG by making use of the following parametrization for the Hagedorn mass spectrum [20];

$$\rho(m) = C \frac{\theta(m - M)}{(m^2 + m_0^2)^a} \exp\Big(\frac{m}{T_H}\Big), \quad (7)$$

where M is the cut-off mass for selected hadrons and T_H is the Hagedorn temperature chosen as 180 MeV for our analysis. For other parameters, we have chosen $C = 0.05$

GeV$^{3/2}$, $m_0 = 0.5$ GeV and $a = 5/4$ [18]. The inclusion of Hagedorn states leads us to adopt Boltzmann approximation. Thus, the previously defined thermodynamic properties are modified as;

$$P^H(T,\mu) = \frac{T}{2\pi^2}\int dm \int_0^\infty p^2 dp\ \exp\Big(-\frac{E-\mu}{T}\Big) \times \Big[\sum_i g_i\delta(m-m_i)+\rho(m)\Big] \tag{8}$$

$$\varepsilon^H(T,\mu) = \frac{1}{2\pi^2}\int dm \int_0^\infty p^2 E\ dp\ \exp\Big(-\frac{E-\mu}{T}\Big) \times \Big[\sum_i g_i\delta(m-m_i)+\rho(m)\Big] \tag{9}$$

$$n^H(T,\mu) = \frac{1}{2\pi^2}\int dm \int_0^\infty p^2 dp\ \exp\Big(-\frac{E-\mu}{T}\Big) \times \Big[\sum_i g_i\delta(m-m_i)+\rho(m)\Big] \tag{10}$$

$$s^H(T,\mu) = \frac{1}{2\pi^2}\int dm \int_0^\infty p^2 dp\ \exp\Big(-\frac{E-\mu}{T}\Big) \times \Big(1+\frac{E-\mu}{T}\Big)\Big[\sum_i g_i\delta(m-m_i)+\rho(m)\Big] \tag{11}$$

Repulsive interactions at short distances are introduced into IHRG by using thermodynamically consistent excluded volume approach [19]. This, in essence, is a van der Waals correction. The system volume V is now replaced by the available volume V_{av},

$$V \to V_{av} = V - \sum_i v_i N_i, \tag{12}$$

where $v_i = 16\pi r_i^3/3$ is the excluded volume parameter (also called as eigen volume) [17, 18] and N_i is the number of particles of type i. From here on, we restrict ourselves to the case of equal volume parameter v_i for all hadrons, $v = 16\pi r_h^3/3$. Use of Eq. 12 in grand canonical ensemble changes pressure through an iterative process [17, 18],

$$P^{ev}(T,\mu) = \kappa P^H(T,\mu), \tag{13}$$

where, κ is the excluded volume suppression factor given by,

$$\kappa = exp\Big(-\frac{vP^{ev}}{T}\Big). \tag{14}$$

Accordingly, the thermodynamic entities like ε, n and s are modified as follows;

$$\varepsilon^{ev}(T,\mu) = \frac{\kappa\varepsilon^H(T,\mu)}{1+\kappa v n^H(T,\mu)} \tag{15}$$

$$n^{ev}(T,\mu) = \frac{\kappa n^H(T,\mu)}{1+\kappa v n^H(T,\mu)} \tag{16}$$

$$s^{ev}(T,\mu) = \frac{\kappa s^H(T,\mu)}{1+\kappa v n^H(T,\mu)}. \tag{17}$$

B. Re, Kn and Ma of the Hadron Gas

The transport properties of hadron gas can be investigated by using the Boltzmann Transport Equation (BTE) which is given by,

$$\frac{\partial f_p}{\partial t} + v_p^i\frac{\partial f_p}{\partial x^i} + F_p^i\frac{\partial f_p}{\partial p^i} = I(f_p), \tag{18}$$

where v_p^i is the velocity of the ith hadron and F_p^i is the external force acting on it. $I(f_p)$ is the collision integral which gives the change of distribution function due to collisions. The thermal equilibrium in a system is achieved and maintained by the collisions among the constituents. Under the relaxation time approximation the collision integral can be written as:

$$I(f_p) = -\frac{(f_p - f_p^0)}{\tau(E_p)}, \tag{19}$$

where $\tau(E_p)$ is the particle dependent relaxation time and f_p^0 is the equilibrium distribution function defined as;

$$f_p^0 = \exp(-\frac{E_i-\mu}{T}). \tag{20}$$

For a hadron gas at finite chemical potential, the shear viscosity can be obtained by using the following expression [21],

$$\eta = \sum_i \frac{1}{15T}\int \frac{d^3p}{(2\pi)^3}\frac{p^4}{E_i^2}(\tau_i f_i^0 + \bar{\tau}_i\bar{f}_i^0) \tag{21}$$

where τ_i is the relaxation time of the hadron i and f_i^0 is its corresponding equilibrium distribution function. The particle-dependent average relaxation time is given by,

$$\tilde{\tau}_i^{-1} = \sum_j n_j\langle\sigma_{ij}v_{ij}\rangle, \tag{22}$$

where n_j is the number density of j^{th} hadronic species, σ_{ij} is the cross section for the interaction between hadron i and j, and v_{ij} is the relative velocity between them. Furthermore, considering hadrons as hard spheres of equal radius r_h (having constant cross section $\sigma = 4\pi r_h^2$), the thermal average of total cross section times relative velocity i.e. $\langle\sigma v\rangle$ can be calculated as [21–23],

$$\langle\sigma_{ij}v_{ij}\rangle = \frac{\int d^3p_i d^3p_j v_{ij}\sigma ij f_i^0 f_j^0}{\int d^3p_i d^3p_j f_i^0 f_j^0} = \sigma\langle v_{ij}\rangle. \tag{23}$$

Now, rewriting the momentum integral in terms of energy of the hadrons and scattering angle θ [21, 24] we get;

$$\langle \sigma_{ij} v_{ij} \rangle = \frac{\sigma \int p_i p_j E_i dE_i E_j dE_j d\cos\theta f_i^0 f_j^0 \times \frac{\sqrt{(E_i E_j - p_i p_j \cos\theta)^2 - (m_i m_j)^2}}{E_i E_j - p_i p_j \cos\theta}}{\int p_i p_j E_i dE_i E_j dE_j d\cos\theta f_i^0 f_j^0} \quad (24)$$

where E_i (E_j) is integrated in the limit m_i (m_j) to ∞, respectively. The limit of integration of $\cos\theta$ runs from -1 to +1. Finally, the relaxation time is calculated using Eqs. 22 and 24.

The Hagedorn states being highly unstable, decay rapidly and it is reasonable to assume that their presence affects the mean free paths of the hadrons in the medium. They also significantly affect the thermodynamics of hadronic matter close to the QCD critical temperature. Hence their contribution cannot be ignored. The contribution from these states to the shear viscosity can be estimated by using the approximation that the mean free path of such resonances is inversely related to their decay widths [25–27]. The decay width of Hagedorn states are obtained by a linear fit to the decay widths of all resonances in the particle data book. Assuming that these particles have hard-core radius r_h, the excluded volume approximated contribution to shear viscosity from Hagedorn states is given by,

$$\eta_H = \frac{5T^{3/2}}{128\pi^{5/2} n^H(T)} \int m^{5/2} dm\ \rho(m) K_{\frac{5}{2}}\left(\frac{m}{T}\right). \quad (25)$$

where $n^H(T)$ is the number density of Hagedorn states in the medium and K_n is the modified Bessel function of the second kind.

The applicability of fluid dynamics in a system can be probed with the help of Kn. A small value for Kn indicates a high degree of thermalization in the system due to frequent collisions between the constituent particles in the medium. The Knudsen number is defined by the ratio of characteristic microscopic to characteristic macroscopic lengths [28],

$$Kn = \frac{\text{microscopic length scale}}{\text{macroscopic length scale}} \quad (26)$$

where the microscopic and the characteristic macroscopic length scales are taken as the mean free path (λ) and the linear dimension of the system (D) respectively. D is the maximum possible value of the macroscopic length scale. In central collisions of identical nuclei the maximum system size may be taken as the diameter of the nuclei however, the size will be smaller in peripheral collisions which depends on the value of the impact parameter. For given λ, this will give the lower bound of Kn, which will help in finding out the domain of application of ideal hydrodynamics ($Kn \to 0$). The first order hydrodynamics $\sim Kn$ and the second order hydrodynamics $\sim Kn^2$, etc. We used the following expression for Kn here,,

$$Kn = \lambda / D, \quad (27)$$

where $\lambda = \frac{1}{\sqrt{2} n^{ev} \sigma}$. The inverse of Kundsen number is a measure of the average number of scattering that a hadron undergoes in the medium.

The choice of characteristic macroscopic length scale as the linear size scale can be justified for a system where the hydrodynamic variables do not change appreciably for length scale smaller than the linear dimension of the system *i.e.* when the gradient of hydrodynamic quantities are small. Such a choice provides the lower bound of Kn and upper bound of Re. For small Kn the ideal hydrodynamics is a good approximation for the description of the system as the first and second order hydrodynamics are proportional to Kn and Kn^2 respectively.

For a fluid with low Kn, the characteristics of the fluid and flow can now be studied by making use of Re and Ma. The Reynold number is defined as [28]:

$$Re = \frac{\text{Inertial force}}{\text{Viscous force}} = \frac{lv\rho}{\eta} \quad (28)$$

where l is the characteristic macroscopic length scale $\sim$ spatial dimension over which hydrodynamic variables do not change appreciably, v is characteristic flow velocity, ρ is the mass density of the fluid and η is the shear viscosity. For relativistic fluid one replaces ρ by $(\epsilon + P) = sT$, where s is the entropy density (for non-zero baryonic chemical potential $\epsilon + P - \mu n = sT$). The Knudsen number is related with the inverse of Reynold number. The characteristic macroscopic length scale l appears through the shear force, $\sim \eta \partial v_i / \partial x_j \sim \eta v / l$ *i.e.* l is to be estimated from the gradient of hydrodynamic quantities, for example, $l^{-1} \sim v^{-1} \partial v / \partial x$. In the present work l is chosen as the linear size (D) of the system *i.e.* $l = D$, which is the maximum possible value of l. This will give maximum value of Re (keeping other parameters fixed) and hence it imposes limit to the laminar flow.

The Reynold number can also be defined as the ratio of thermodynamic pressure (P) to bulk viscous pressure (Π) and thermodynamic pressure to the magnitude of shear stress tensor ($\pi^{\mu\nu}$) as [29, 30]: $R_\Pi = (\epsilon + P)/\Pi$ and $R_\pi = (\epsilon + P)/\sqrt{\pi_{\mu\nu}\pi^{\mu\nu}}$ respectively which can be estimated realistically by solving hydrodynamic equations for an expanding system formed in heavy ion collisions.

Following simple ideal equation of state $\varepsilon = 3P$, a limit on Reynold number can be imposed using causality [31]. We estimate the Re by using the expression given below,

$$Re = \frac{D\langle v \rangle T}{\eta / s^{ev}}, \quad (29)$$

where $\langle v \rangle$ is the average of characteristic flow velocity as described below. The expansion velocity of the fluid can

be defined as [32]:

$$v_{\rm fluid}(t,\vec{r}) = \int \frac{d^3p}{(2\pi)^3}\frac{\vec{p}}{E}f(E) / \int \frac{d^3p}{(2\pi)^3}f(E) \qquad (30)$$

In the non-relativistic domain, $\vec{p}/E$ may be replaced by $\vec{p}/m$. The velocity of the particles (hadrons here) in the co-moving frame (v') is connected with the velocity in the laboratory frame (v) through Lorentz transformation by the fluid velocity ($v_{\rm fluid}$). The average of v' is zero but not the average of v. In eq. 30 $f(E)$ is the phase space distribution in the co-moving frame which can be replaced by local equilibrium distribution as a leading order approximation with space-time dependent temperature and chemical potential. For the purpose of estimating Re one may take the space-time average of $v_{\rm fluid}$ weighted by energy density of the fluid to get $\langle v\rangle$. However, in the present work, the hydrodynamic equations are not solved to get fluid velocity, therefore, we take this as a parameter. It may be mentioned here that the average velocity of the fluid at rest may be non-zero for non-central collision as indicated in Ref. [33]. We take different values of $\langle v\rangle = 0.3c, 0.5c$ and $0.7c$ (see also [33]) to understand the sensitivity of the results on the fluid velocity. The results are shown with $\langle v\rangle = 0.5c$, which is in agreement with the values that can be estimated by using Eq.30 for the chosen range of temperature. The viscous correction to the distribution function has been neglected as it is found to be small [34]. A high value of Re is usually associated with the turbulence in the medium thereby creating eddies and through small eddies energy dissipation takes place in the fluid. In the above two cases, we have used D as the characteristic length scale. This necessarily means that we have only two length scales which are: the system dimension D and mean free path λ. Therefore, in principle, the length scale that appears in the expression for Re must be more than λ and its upper limit should be D.

Finally, the Ma combines the fluid velocity and the speed of sound in the system and is written as,

$$Ma = \langle v\rangle / c_s, \qquad (31)$$

where

$$c_s^2 = \frac{\frac{\partial P}{\partial T} + \frac{\partial P}{\partial \mu_B}\frac{d\mu_B}{dT}}{\frac{\partial \varepsilon}{\partial T} + \frac{\partial \varepsilon}{\partial \mu_B}\frac{d\mu_B}{dT}}, \qquad (32)$$

is the speed of sound in the system which reduces to $c_s^2 = (\frac{\partial P}{\partial \varepsilon})$ at vanishing baryon chemical potential. Here,

$$\frac{d\mu_B}{dT} = \frac{s\frac{\partial n}{\partial T} - n\frac{\partial s}{\partial T}}{n\frac{\partial s}{\partial \mu_B} - s\frac{\partial n}{\partial \mu_B}}. \qquad (33)$$

The Re, Kn and Ma obey the following relation [16]:

$$Re \times Kn = v\lambda\frac{\rho}{\eta} = \frac{v}{c_s} = Ma \qquad (34)$$

where we have used $\eta/\rho = \lambda c_s$ to obtain the above relation. This indicates the Mach number, Ma is independent of length scale.

A small value of Ma is usually associated with the incompressibility of the medium. It may be mentioned here that Re and Ma are independent of each other as one of them depends on the macroscopic dimension of the system. The Ma would thus give similar results over different system sizes provided that the other available conditions are identical.

With the help of the formulae given above, we now move forward to estimate the dimensionless parameters Re, Kn and Ma.

III. RESULTS AND DISCUSSION

We include all the hadrons and resonances up to a mass of 2.25 GeV listed in the particle data book [35] along with the Hagedorn spectrum. The thermodynamic properties are dependent on the eigen volume of hadrons which have to be chosen appropriately. It is dependent only on the unknown parameter r_h. The hadron-hadron interactions are not repulsive for an r_h value comparable to the charge radii. Hence, it was argued that r_h should be taken according to the hard-core radius known from nucleon-nucleon scattering. The repulsive interactions are mediated by ω mesons and the range of interaction is inversely proportional to the mass of the mediator. Based upon the above argument, we have chosen a hard-core radius, $r_h = 0.3$ fm, to incorporate the repulsive interaction. Also, there is not much deviation in charge radii between baryons and mesons, therefore, uniform hard-core radius ($r_h = 0.3$ fm) is considered for all hadrons [21, 24, 36].

The effect of system size on volume and particle numbers, considered infinite in the thermodynamic limit, can be implemented by providing a lower momentum cut-off to the integral over momentum space [37–39]. The finite-size effect is introduced by using a lower limit of momentum $p_{\rm cutoff}({\rm MeV}) = 197\pi/D({\rm fm})$ [39]. Here $D = 2R$ is the characteristic system size, R being the system radius. We chose a few representative radii, R = 1.5, 3, 5, 7 and 10 fm to cover system properties from high multiplicity pp to ultra-relativistic heavy-ion collisions based on experimentally obtained HBT radii [39–43]. This choice of system size goes inline with the recent observations of finite hadronic phase lifetime observed in pp and heavy-ion collisions [44, 45].

To validate our study, we have compared our results with others in Fig. 1. It shows the dependence of η/s on system temperature for a fixed system size at zero chemical potential ($\mu_B = 0.0$ GeV). The AdS/CFT bound of η/s (also known as KSS limit), which is $1/4\pi$ [1], is also shown in the figure. It is observed that the η/s in the given temperature range of the hadronic

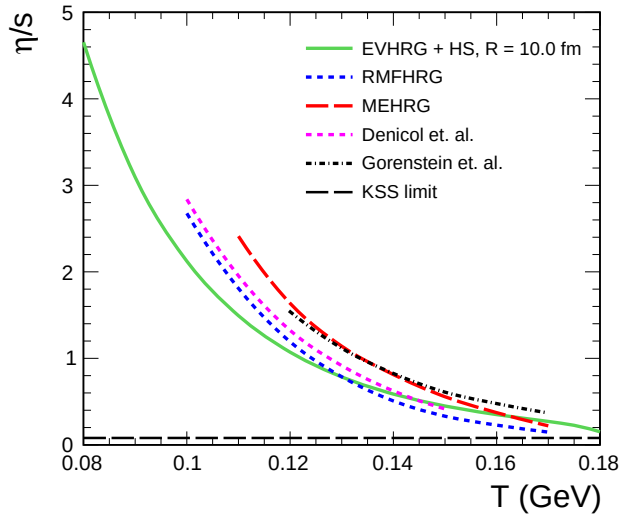

FIG. 1: Comparison of η/s obtained for $R = 10.0$ fm with the estimations of other models at $\mu_B = 0.0$ GeV [25, 46–48].

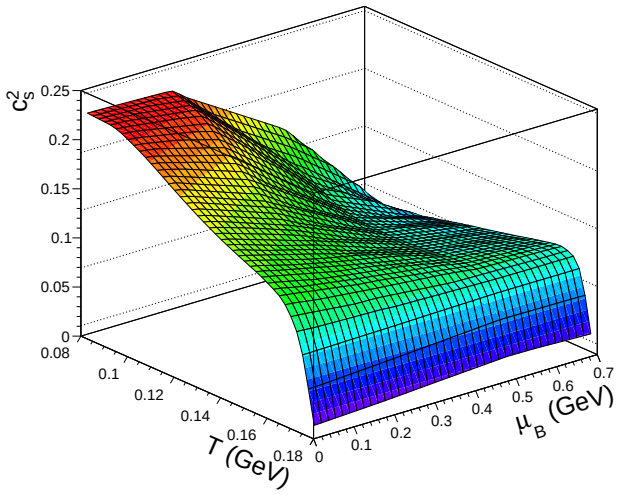

FIG. 3: The c_s^2 as a function of temperature and μ_B for $R = 10.0$ fm.

phase shows a near-perfect fluid behavior towards higher temperatures. Our study is in good agreement with the values of η/s obtained by Gorenstein et al., where the authors considered EVHRG within relativistic molecular kinetic theory [46]. We have also compared our η/s values with the results obtained from Chapman-Enskog theory, relativistic mean-field HRG and EVHRG formalism with Hagedorn spectrum [25, 47, 48].

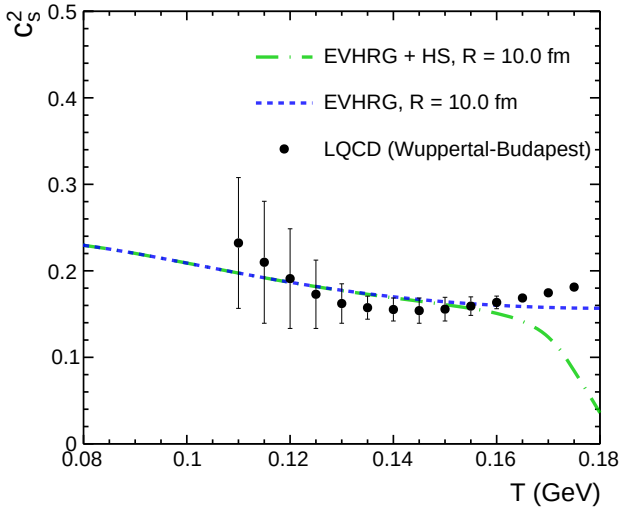

FIG. 2: The square of the speed of sound (c_s^2) as a function of temperature (T). This is compared with lattice data [49].

Further, the dependence of the speed of sound on temperature is compared with lattice QCD data at $\mu_B = 0.0$ GeV in Fig. 2. It is observed that c_s^2 obtained in EVHRG formalism is in agreement with the LQCD data except at the high-temperature regime [49], where the HRG model is not a good approximation for the description of the system. The addition of the Hagedorn spectrum accentuates this deviation because of the rapid increase in energy density as compared to the pressure on approaching the Hagedorn temperature.

In Fig. 3 the variation of c_s^2 is explored with temperature (T) and chemical potential (μ_B). We have observed that increasing temperature at very low chemical potential ($\mu_B = 0 - 0.2$ GeV) gives similar results as discussed in Fig. 2. However, at $\mu_B > 0.2$ GeV with increasing T speed of sound squared (c_s^2) decreases initially up to $T \sim 0.140$ GeV and then start increasing with temperature. As μ_B increases the dip in c_s^2 shifts towards the lower T. This smooth change in the behaviour of c_s^2 with high μ_B mimics the phase transition at $T < T_c \approx 0.160$ GeV. The sudden drop in the c_s^2 at high T is caused by the same effect of the Hagedorn states as seen in Fig. 2.

Large values of Kn, imply that the system is far from thermodynamic equilibrium, while small values (tending to zero), indicate a high degree of thermalization. Fig. 4 shows the dependence of Kn on system radius. We observe a small value of Kn at low temperatures for large R. This indicates that larger systems have a higher tendency to achieve thermodynamic equilibrium as the hadrons undergo larger number of collisions. The Kn is small at high temperatures and does not vary much with system radius. This behavior is expected because at lower temperatures the mean free path (λ) is larger, indicating less interaction among the hadrons. The variation of Kn also indicates that the system formed at high tempera-

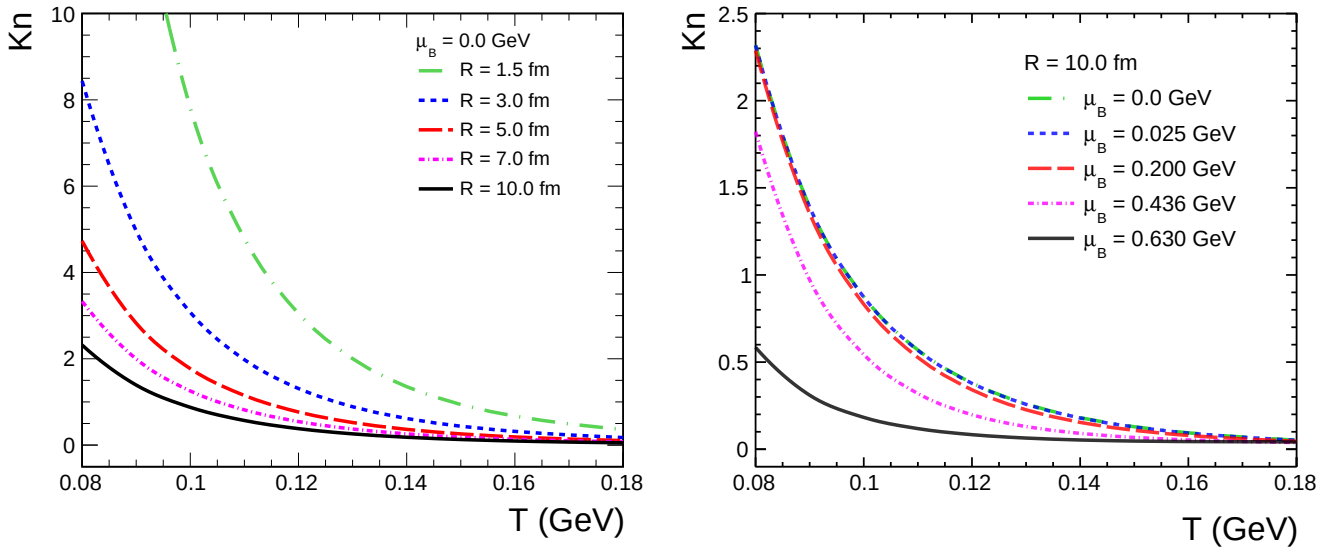

FIG. 4: Knudsen number, Kn, as a function of temperature for different values of system size, R at $\mu_B = 0.0$ GeV (left panel) and for different values of μ_B at $R = 10.0$ fm, which is the case of larger systems (right panel).

tures is close to equilibrium (even for the lowest value of $R = 1.5$ fm considered here) and therefore, we can apply hydrodynamics to study the evolution of the system. The variation of Kn as a function of temperature for different chemical potentials is also shown in the right panel of Fig. 4. We see that Kn decreases with an increase in μ_B.

Re, is an important parameter in hydrodynamics that contains information regarding instabilities in the fluid. A high value of Re is usually associated with turbulence in the fluid. The inverse of Reynolds number, Re^{-1}, is generally seen as a proxy for η/s in ultra-relativistic heavy-ion collisions as both of them are directly related. As a result of this relation, $Re >> 1$ implies flow with low viscosity. We present the dependence of Re on system size in Fig. 5. We note that it increases with temperature for all values of R, indicating that the system becomes less viscous at higher temperatures and approaches a 'perfect fluid' limit. Fig. 5 also explores the variation of Re with chemical potential (right panel). We have chosen five different values of chemical potentials; $\mu_B = 0.0$, 0.025, 0.200, 0.436, and 0.630 GeV, which corresponds to LHC energies, RHIC at $\sqrt{s_{\rm NN}} = 200$ GeV and $\sqrt{s_{\rm NN}} = 19.6$ GeV, RHIC/FAIR at $\sqrt{s_{\rm NN}} = 7.7$ GeV and NICA at $\sqrt{s_{\rm NN}} = 3$ GeV respectively [50–53]. The system radius is fixed at 10.0 fm, which roughly corresponds to ultra-relativistic heavy-ion collisions. At low temperatures, Re increases with μ_B indicating that the viscosity of the system decreases with increasing μ_B. As it appears, at higher temperature the Re, becomes almost independent of the baryochemical potential of the system. The flow becomes turbulent for large $Re \gtrsim 2000$ [54]. The values of Re obtained here indicate that the flow is laminar for the system under consideration. However, there may be other kinds of instabilities in the system for small Re, like Kelvin-Helmholtz type [33].

Supersonic flows significantly impact two-particle correlations because of the formation of Mach cones. The interest in Mach cones formed in ultra-relativistic heavy-ion collisions was sparked from the two-particle correlations observed at RHIC [55, 56]. However, subsequent measurements at the LHC energies do not support these observations [57, 58]. It is argued that the structure observed might be an artefact of incorrect background considerations [59]. Although there is no direct experimental evidence for their existence, theoretical interest in Mach cones still persists as their disappearance could hint at a possible QCD critical point [60]. The dependence of Ma on c_s makes it sensitive to the critical point (CP). If $Ma << 1$, the density is almost uniform throughout the system and the fluid is incompressible indicating a very low bulk viscosity. Fig. 6 depicts the variation of Ma with system radius. We observe that Ma is almost independent of system radii beyond a particular temperature as expected with small deviations only due to the lower momentum cut-off. As temperature increases, it is observed that Ma increases.

It was observed that as η/s increases, the typical Mach cone structure smears out and vanishes [61, 62]. Right panel of Fig. 6 displays the dependence of Ma on μ_B. We see that it increases with increasing μ_B and remains above the supersonic limit at all temperatures considered here. This might be an indication of the early formation of a rapidly expanding system with shock waves at higher μ_B values. From Fig. 6, it can also be inferred that since Ma is greater than unity at all temperatures for all values

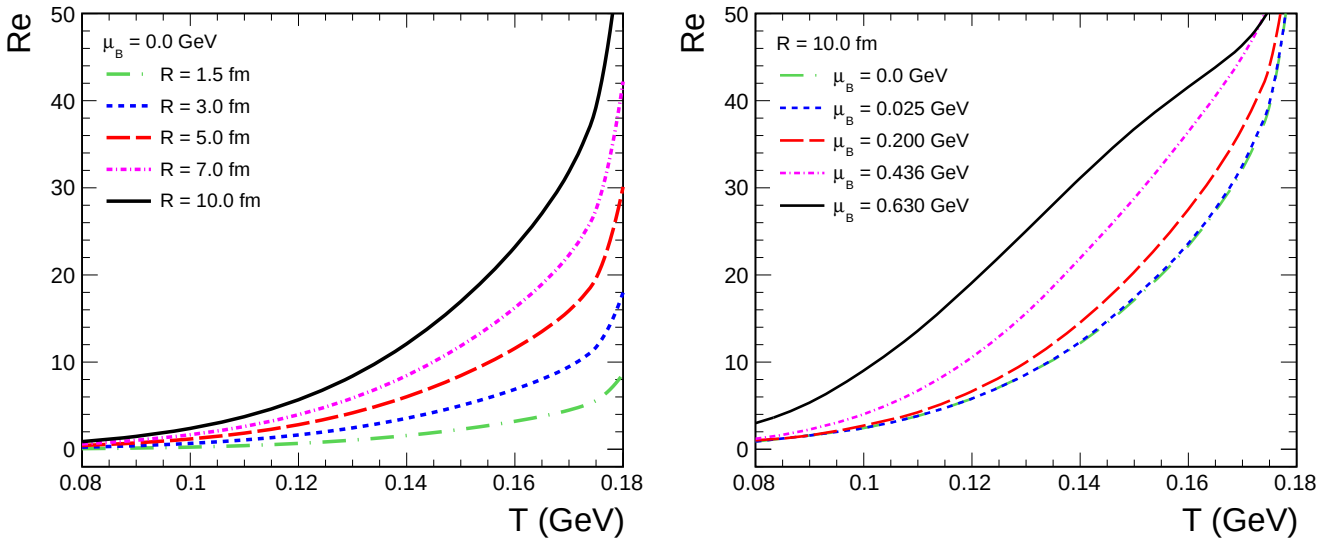

FIG. 5: Reynolds number as a function of temperature for different values of R at $\mu_B = 0$ GeV (left panel) and different values of μ_B at $R = 10.0$ fm, which is the case of heavy-ion collisions (right panel).

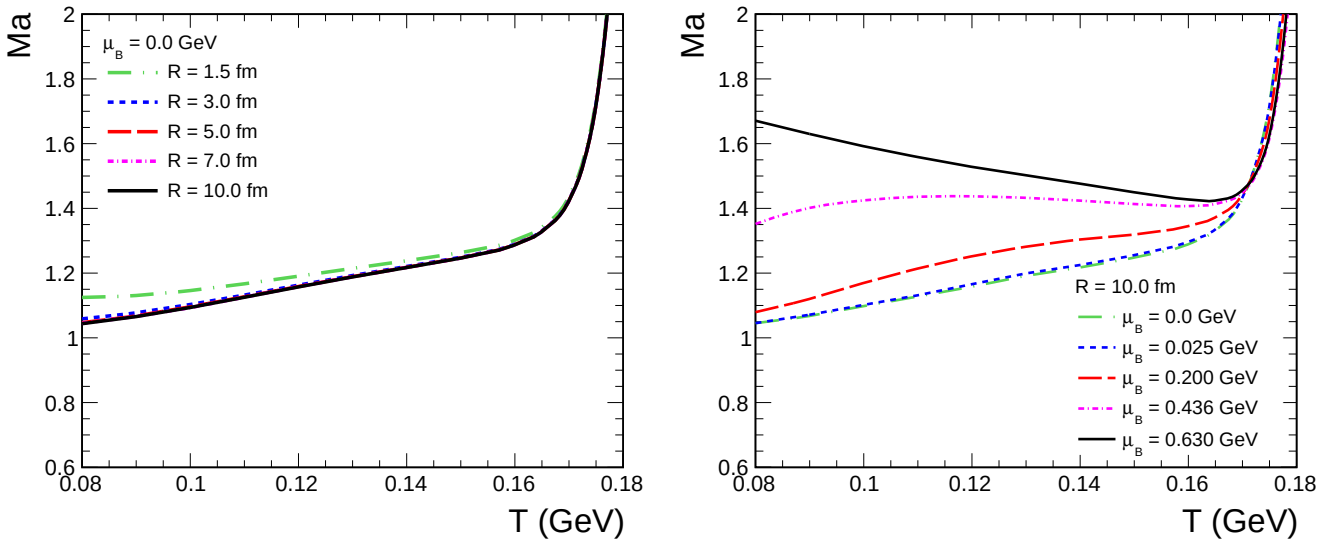

FIG. 6: Mach number, Ma, as a function of temperature for different values of system size, R at $\mu_B = 0.0$ GeV (left panel) and for different values of μ_B at $R = 10.0$ fm, for larger systems (right panel).

of μ_B considered here, indicating that the system produced in ultra-relativistic collisions is compressible [16].

Fig.7 depicts the effect of the magnitude of the fluid velocity chosen here. It is observed that the qualitative dependence of Ma on temperature remain unchanged. We can also deduce that the hadronic fluid considered is compressible for all values of fluid velocity greater than $0.5c$. At lower velocities, the hadronic fluid is incompressible at low temperatures. A similar scaling can also be expected for Re as $Re \propto \langle v \rangle$ as seen in Eq.29.

IV. SUMMARY

In summary, we have estimated various relevant parameters like Re, Kn and Ma which assist in characterizing many-particle system. The dependence of these parameters on the system size, temperature, chemical potential for hadrons produced in ultra-relativistic nuclear collisions have been investigated. The obtained values ($Kn << 1$, $Ma \sim 1$ and $Re >> 1$) indicate the occurrence of compressible low viscous flows at high temperatures close to the phase transition region ($T \sim 150 - 170$

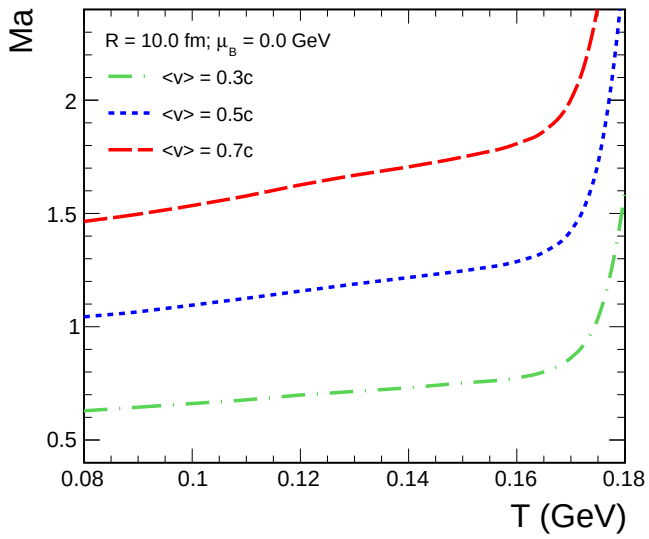

FIG. 7: The effect of variation of the fluid velocity parameter, $\langle v \rangle$, is shown. It is observed that a change in $\langle v \rangle$ results only in a scaling of the values without any change in the qualitative nature of the results.

MeV). The degree of thermalization of hadron gas estimated is comparable over different system sizes, hinting for the justification of the application of hydrodynamics in interpreting the results from high multiplicity pp to heavy-ion collisions. This puts into question the applicability of pp collisions as a baseline for heavy-ion collisions at the high beam energies presently accessible at different particle accelerators.

Relativistic second-order causal viscous hydrodynamics [63] is used extensively to analyze the system formed in nuclear collisions at relativistic energies, because the relativistic generalization first order (Navier-Stokes) hydrodynamics is acausal and it gives rise to unstable solutions. Application of second-order hydrodynamics needs shear and bulk viscous coefficients, thermal conductivity, and various relaxation and coupling coefficients. That is the second-order hydrodynamics introduces more unknown coefficients as inputs than its first-order version. Fluid dynamics can also be applied to systems away from equilibrium by including higher order gradients of hydrodynamic quantities [12]. The inclusion of the order of these gradients will depend on how far away the system remains from equilibrium. The higher order gradients can be ignored for systems that are close to the equilibrium and hence a smaller number of transport coefficients will suffice to characterize it. We have estimated here the Kn to examine the applicability of the hydrodynamics, Ma to determine whether the fluid is compressible or incompressible. In the relativistic domain, the fluid is compressible and hence the bulk viscous coefficient will be required as input for hydrodynamic simulation. The Re decides whether the flow is laminar or turbulent. For turbulent flow inclusion of higher-order gradients will be crucial. We have assumed that the hydrodynamic quantities change appreciably only over the linear dimension of the system. This assumption helps us to choose the characteristic macroscopic length scale as the linear dimension of the system for estimating Kn and Re. Such a choice sets the lower and upper bound on Kn and Re respectively when other parameters (mean free path, average velocity, shear viscosity, etc.) are kept fixed. These bounds will be useful to figure out the applicability of ideal hydrodynamics. Therefore, the estimates of Kn, Re, and Ma from analysis of data will be useful to understand fluid in a comprehensive manner.

Acknowledgment

This research work has been carried out with financial support from DAE-BRNS, the Government of India, Project No. 58/14/29/2019-BRNS of Raghunath Sahoo. For the research fellowship, Ronald Scaria acknowledges CSIR, Govt. of India. CRS and RS acknowledge the financial support under the above BRNS project. Further R.S. acknowledges the financial support under the CERN Scientific Associateship, CERN, Geneva, Switzerland. The authors acknowledge the Tier-3 computing facility in the experimental high-energy physics laboratory of IIT Indore supported by the ALICE project.

[1] P. Kovtun, D. T. Son and A. O. Starinets, Phys. Rev. Lett. **94**, 111601 (2005).
[2] I. Arsene et al. (BRAHMS Collaboration), Nucl. Phys. A **757**, 1 (2005).
[3] B. B. Back et al. (PHOBOS Collaboration), Nucl. Phys. A **757**, 28 (2005).
[4] J. Adams et al. (STAR Collaboration), Nucl. Phys. A **757**, 102 (2005).
[5] K. Adcox et al. (PHENIX Collaboration), Nucl. Phys. A **757**, 184 (2005).
[6] J. Adam et al. (ALICE Collaboration), Nat. Phys. **13**, 535 (2017).
[7] V. Khachatryan et al. (CMS Collaboration), Phys. Lett. B **765**, 193 (2017).
[8] D. Velicanu [CMS Collaboration], J. Phys. G **38**, 124051 (2011).
[9] R. Campanini and G. Ferri, Phys. Lett. B **703**, 237 (2011).
[10] D. Thakur, S. De, R. Sahoo and S. Dansana, Phys. Rev. D **97**, 094002 (2018).
[11] D. Sahu, S. Tripathy, R. Sahoo and S. K. Tiwari, Eur. Phys. J. A **58**, 78 (2022).
[12] P. Romatschke and U. Romatschke, *Relativistic Fluid Dynamics In and Out of Equilibrium*, Cambridge Uni-

versity Press (2019).
[13] R. S. Bhalerao, J. P. Blaizot, N. Borghini and J. Y. Ollitrault, Phys. Lett. B **627**, 49 (2005).
[14] H. J. Drescher, A. Dumitru, C. Gombeaud and J. Y. Ollitrault, Phys. Rev. C **76**, 024905 (2007).
[15] W. T. Deng and X. G. Huang, Phys. Rev. C **93**, 064907 (2016).
[16] J-Y Ollitrault, Eur. J. Phys. **29**, 275 (2008).
[17] A. Andronic, P. Braun-Munzinger, J. Stachel, and M. Winn, Phys. Lett. B **718**, 80 (2012).
[18] V. Vovchenko, D. V. Anchishkin, and M. I. Gorenstein, Phys. Rev. C **91**, 024905 (2015).
[19] D. H. Rischke, M. I. Gorenstein, H. Stöcker, W. Greiner, Z. Phys. C **51**, 485 (1991).
[20] R. Hagedorn and J. Ranft, Nuovo Cim. Suppl. **6**, 169 (1968).
[21] G. P. Kadam and H. Mishra, Phys. Rev. C **92**, 035203 (2015).
[22] Mirco Cannoni, Phys. Rev. D **89**, 103533 (2014).
[23] P. Gondolo and G. Gelmini, Nucl. Phys. B **360**, 145 (1991).
[24] S. K. Tiwari, S. Tripathy, R. Sahoo and N. Kakati, Eur. Phys. J. C **78**, 938 (2018).
[25] G. Kadam and S. Pawar, Adv. High Energy Phys. **2019**, 6795041 (2019).
[26] J. Noronha-Hostler, J. Noronha, and C. Greiner, Phys. Rev. C **86**, 024913 (2012).
[27] J. Noronha-Hostler, J. Noronha, and C. Greiner, Phys. Rev. Lett. **103**, 172302 (2009).
[28] L. D. Landau and E. M Lifshitz, *Fluid Mechanics*, Pergamon Press (1987).
[29] G. S. Denicol, H. Niemi, E. Molnár, and D. H. Rischke Phys. Rev. D **85**, 114047 (2012) [E: Phys. Rev. D 91, 039902 (2015)].
[30] B. Betz, D. Henkel and D.H. Rischke, Prog. Part. Nucl. Phys., **62**, 556 (2009).
[31] C. Chiu and C. Shen, Phys. Rev. C **103**, no.6, 064901 (2021)
[32] E. M. Lifshitz and L. P. Pitaevskii, *Physical Kinetics*, Butterworth-Heinemann Ltd. (1981).
[33] L. P. Csernai, D. D. Strottman and Cs. Androlik, Phys. Rev. C **85**, 054901 (2012).
[34] A. Monnai, S. Mukherjee, and Y. Yin, Phys. Rev. C 95, 034902 (2017).
[35] P.A. Zyla et al. (Particle Data Group), PTEP **2020**, no.8, 083C01 (2020).
[36] P. Braun-Munzinger, I. Heppe, J. Stachel, Phys. Lett. B **465**, 15 (1999).
[37] K. Redlich and K. Zalewski, arXiv:1611.03746 (2016).
[38] A. Bhattacharyya, R. Ray, S. Samanta and S. Sur, Phys. Rev. C **91**, 041901(R) (2015).
[39] N. Sarkar and P. Ghosh, Phys. Rev. C **96**, 044901 (2017).
[40] K. Aamodt *et al.* [ALICE], Phys. Rev. D **84**, 112004 (2011).
[41] J. Adam *et al.* [ALICE], Phys. Rev. C **91**, 034906 (2015).
[42] S. Acharya *et al.* [ALICE], Phys. Rev. C **100**, 024002 (2019).
[43] S. Chatterjee, S. Das, L. Kumar, D. Mishra, B. Mohanty, R. Sahoo and N. Sharma, Adv. High Energy Phys. **2015**, 349013 (2015).
[44] D. Sahu, S. Tripathy, G. S. Pradhan and R. Sahoo, Phys. Rev. C **101**, 014902 (2020).
[45] S. Acharya *et al.* [ALICE], Phys. Lett. B **802**, 135225 (2020).
[46] M. Gorenstein, M. Hauer, O. Moroz, Phys.Rev.C **77**, 024911 (2008).
[47] G.S. Denicol, C. Gale, S. Jeon, and J. Noronha, Phys. Rev. C **88**, 064901 (2013).
[48] G. Kadam and H. Mishra, Phys. Rev. D **100**, 074015 (2019).
[49] S. Borsányi, Z. Fodor, C. Hoelbling, S. D. Katz, S. Krieg, K. K. Szabó, Phys. Lett. B **730**, 99 (2014).
[50] N. A. Tawfik, L. I. Abou-Salem, A. G. Shalaby, M. Hanafy, A. Sorin, O. Rogachevsky and W. Scheinast, Eur. Phys. J. A **52**, 324 (2016).
[51] P. Braun-Munzinger, D. Magestro, K. Redlich and J. Stachel, Phys. Lett. B **518**, 41 (2001).
[52] J. Cleymans, H. Oeschler, K. Redlich and S. Wheaton, Phys. Rev. C **73**, 034905 (2006).
[53] A. Khuntia, S. K. Tiwari, P. Sharma, R. Sahoo and T. K. Nayak, Phys. Rev. C **100**, 014910 (2019).
[54] B. McInnes, Nucl. Phys. B **921**, 39 (2017).
[55] M. M. Aggarwal et al. (STAR collaboration), Phys. Rev. C **82**, 024912 (2010).
[56] A. Adare et al. (PHENIX collaboration), Phys. Rev. Lett. **104**, 252301 (2010).
[57] G. Aad et al. (ATLAS collaboration), Phys. Lett. B. **739**, 320 (2014).
[58] S. Chatrchyan et al. (CMS collaboration), Phys. Rev. C. **90**, 024908 (2014).
[59] C. Nattrass, N. Sharma, J. Mazer, M. Stuart and A. Bejnood, Phys. Rev. C. **94**, 011901 (2016).
[60] G. Sarwar, M. Hasanujjaman, M. Rahaman, A. Bhattacharyya and J. Alam, Phys. Lett. B **820**, 136583 (2021).
[61] I. Bouras, A. El, O. Fochler, H. Niemi, Z. Xu and C. Greiner, Phys. Lett. B **710**, 641 (2012) [E: Phys. Lett. B **728**, 156 (2014)].
[62] I Bouras et al, J. Phys.: Conf. Ser. **270**, 012012 (2011).
[63] W. Israel and J. M. Stewart, Annals Phys., **118**, 341 (1979).